Article

Preliminary Study on Electrodeposition of Copper Platings and Codeposition of Carbon Nanotubes from Organic Solvent

Jae-Hyeok Park [1], Yusei Fujita [2], Takeshi Hagio [1,3,*], Vanpaseuth Phouthavong [3,4], Yuki Kamimoto [1,5], Takeshi Bessho [1] and Ryoichi Ichino [1,3]

[1] Institute of Materials Innovation, Institutes of Innovation for Future Society, Nagoya University, Furo-cho, Chikusa-ku, Nagoya 464-8601, Japan; park.jae.hyeok@mirai.nagoya-u.ac.jp (J.-H.P.); y-kamimoto@uhe.ac.jp (Y.K.); ichino.ryoichi@material.nagoya-u.ac.jp (R.I.)
[2] Department of Materials, Physics and Energy Engineering, Graduate School of Engineering, Nagoya University, Furo-cho, Chikusa-ku, Nagoya 464-8603, Japan
[3] Department of Chemical Systems Engineering, Graduate School of Engineering, Nagoya University, Furo-cho, Chikusa-ku, Nagoya 464-8603, Japan; phouthavong.vanpaseuth.p9@s.mail.nagoya-u.ac.jp
[4] Department of Chemistry, Faculty of Natural Sciences, National University of Laos, P.O. Box 7322, Vientiane 01170, Laos
[5] Department of Environmental Science, Faculty of Human Environment, University of Human Environments, Okazaki 444-3505, Japan
* Correspondence: hagio@mirai.nagoya-u.ac.jp; Tel.: +81-52-747-6594

Abstract: Metal/carbon composite plating is an effective strategy for improving and adding properties to metal plating by incorporating carbon materials into the metal matrices. Copper (Cu) is widely applied, particularly in the areas of heat management and electronic packaging owing to its high thermal and electrical conductivities, which can be further improved together with improvements in mechanical properties by compositing it with carbon nanotubes (CNTs). However, because hydrophobic CNTs are hardly dispersible in aqueous solutions, additional intense acid treatment or the addition of dispersants is required for their dispersion. Moreover, previous studies have reported that these methods suffer from deterioration of composite material performance through the destruction of the CNT surface or the inclusion of dispersants into the plating. Therefore, in this study, the electrodeposition of a Cu/CNT composite in a non-aqueous solvent that can disperse CNTs without any additional treatment is investigated. The experimental results show that it is possible to deposit Cu from a *N*-methyl-2-pyrrolidone containing copper iodide and potassium iodide. Furthermore, Cu/CNT composite platings containing CNTs up to 0.12 mass% were prepared by constant current electrolysis, and applying pulse electrolysis can increase the CNTs content up to 0.22 mass%.

Keywords: carbon nanotubes; copper plating; composite plating; electrodeposition; non-aqueous solvent

Citation: Park, J.-H.; Fujita, Y.; Hagio, T.; Phouthavong, V.; Kamimoto, Y.; Bessho, T.; Ichino, R. Preliminary Study on Electrodeposition of Copper Platings and Codeposition of Carbon Nanotubes from Organic Solvent. *Coatings* **2023**, *13*, 802. https://doi.org/10.3390/coatings13040802

Academic Editor: JongHyeon Lee

Received: 15 March 2023
Revised: 6 April 2023
Accepted: 19 April 2023
Published: 20 April 2023

Copyright: © 2023 by the authors. Licensee MDPI, Basel, Switzerland. This article is an open access article distributed under the terms and conditions of the Creative Commons Attribution (CC BY) license (https://creativecommons.org/licenses/by/4.0/).

1. Introduction

Electrodeposition of metal platings accompanied by the codeposition of carbon materials, namely metal/carbon composite platings, has garnered reputation as a promising method for enhancing the properties or imparting additional functions to conventional metal platings [1,2]. In particular, the codeposition of carbon materials has been found to be an effective strategy for improving corrosion resistance [2–4], electrical conductivity [4,5], thermal conductivity [6–8], abrasion resistance [8,9], hardness [8–10], etc. Numerous carbon materials, including carbon black [11], carbon fibers [12,13], single- or multi-walled carbon nanotubes (CNTs) [2,4,5,9,10,14], graphene and its derivatives [3,8,15,16], and diamonds [6,7,17–19] have been considered as filler materials for composite platings. Although several carbon filler materials are in use, an appropriate carbon material should be chosen according to the desired performance of the plating and environment where it will be used [2].

CNTs have received considerable attention since their discovery as materials with excellent mechanical features, such as their high tensile strength, high elastic modulus) and high conductivity of heat and electricity in the axial direction [2,20]. The one-dimensional fibrous shape and distinctive properties of CNTs generally result in composite platings with unique properties compared with other composite platings using insulating particles as the filler material [9]. In addition, CNT fillers impart improved corrosion resistance owing to their hydrophobicity [21,22] that is different from the mechanism of graphene and its derivatives, which are predominantly based on chemical inertness, obstructing the passage of corrosive media [23,24]. Owing to these unique properties, metal/CNT composite platings have become one of the most intensively studied areas in this field, and various composite platings with high strength, thermal conductivity, abrasion resistance, field-emission element performance, good electrical contact, and electromagnetic wave-shielding performance have been developed [9].

Copper (Cu)/CNTs composite platings are among the most extensively studied metal/CNT systems [5,9,10,14]. Numerous researchers have attempted to develop Cu/CNT composite platings as advanced alternatives to pure Cu, which is widely applied in areas such as mechatronics, aircraft manufacturing, and electrical automation [25]. In particular, Cu/CNT composite platings have grown rapidly in the fields of heat management and electronic packaging owing to their low thermal expansion coefficient, high thermal conductivity, and high carrier density [26]. Furthermore, recent studies have revealed its potential application as a current collector at the anode of lithium batteries [27,28]. To maximize the performance of these Cu/CNT composite platings, a uniform distribution of CNTs in the Cu matrix is essential; this dispersion is regarded as a major challenge in fabricating Cu/CNT composite platings [29].

The homogeneous dispersion of CNTs in plating baths is critical for the fabrication of high-performance Cu/CNT composite platings with a uniform distribution of CNTs [30]. However, as pristine CNTs are hydrophobic, they cannot be dispersed in aqueous plating baths [9]; therefore, various methods have been developed to disperse CNTs in aqueous Cu plating baths. One method involves the addition of dispersants, such as poly(acrylic acid) [31–33], sodium dodecyl sulfate [20], stearyltrimethylammonium bromide [34], and non-ionic dispersants [35]. However, dispersants are not always effective in improving plating properties by codeposition of CNTs through electrochemical deposition. Arai et al. reported that excess amounts of dispersants cause the deterioration of plating properties, such as electrical and thermal conductivities, due to the incorporation of dispersants into the Cu matrix during electrodeposition [31]. The selection of appropriate types and amounts of dispersants is essential for their utilization; however, drawbacks owing to their inclusion into the Cu matrix remain an issue. Another method involves directly functionalizing the surface of the CNTs with hydrophilic functional groups via intense acid treatment [14,25,36]. Most researchers have subjected CNTs to a mixture of sulfuric and nitric acids and treated them at temperatures up to 100 °C. Li et al. treated the CNTs with a mixture of sulfuric and nitric acids at a mixing ratio of 3:1 (v/v) at 50–80 °C for 4–8 h and obtained well-dispersed CNTs in a bath containing $CuSO_4$ [25]. The obtained Cu/CNT composite platings exhibit superior electrical conductivity and mechanical properties. Although functionalization by chemical treatment is an effective way to achieve dispersion, it introduces defects by destroying the sp2 carbon bonding of the CNT surfaces [9,14], thereby causing a deterioration in some properties. Other methods include the electrostatic repulsion of negatively charged CNTs by preparing anionic forms of Cu using complexing agents, such as ethylenediaminetetraacetic acid [30], mechanical agitation, and ultrasonication [37]. Combinations of these methods have also been reported previously [38].

Although a variety of approaches have been adopted, previous studies have primarily focused on enabling the dispersion of CNTs in general $CuSO_4$ aqueous solutions and rarely consider the possibility of using non-aqueous baths that allow the homogeneous dispersion of hydrophobic CNTs without any treatment or dispersants. Pech-Rodríguez et al. reported the possibility of using a eutectic solvent as a plating bath for Cu/CNT composite platings;

however, because eutectic solvents are ionic, they required prior functionalization of the CNTs [39].

In this study, we carried out a preliminary experiment aimed at developing a novel non-aqueous organic Cu plating bath and considered the possibility of preparing Cu/CNT composite platings without the use of dispersants or surface treatments on the CNTs. A suitable organic solvent for CNT dispersion was considered, and the optimal conditions for preparing Cu/CNT composite platings by electrodeposition were explored.

2. Materials and Methods

2.1. Materials

N-methyl-2-pyrrolidone (NMP, ≥99.5%) and potassium iodide (KI, ≥99.9%) were purchased from Kishida chemical Co., Ltd., Osaka, Japan. Dimethyl sulfoxide (DMSO, ≥99.9%), N,N-dimethylformamide (DMF, ≥99.7%), benzene (≥99.0%), acetonitrile (≥99.8%), ethanol (≥99.5%), copper(I) iodide (CuI, ≥98.0%), sodium polyacrylate, molecular sieves (beads, approximately 2 mm), and nitric acid (HNO_3, 60–61%) were purchased from Nacalai Tesque, Kyoto, Japan. All organic solvents were dehydrated by adding 50 g of molecular sieves 4A in 500 mL of organic solvents followed by shaking for 24 h and storage in argon (Ar) atmosphere just before usage to ensure the removal of water. Multi-walled CNTs (MWCNTs; AMC®, diameter of approximately 11 nm, length of approximately 1 μm) were purchased from UBE Corporation, Tokyo, Japan. The metal catalysts of the MWCNTs were removed by stirring 10 g of MWCNTs in 500 mL of 8 mass% HNO_3 solution for 24 h at around 25 °C, followed by filtering, rinsing with distilled water, and drying prior to usage. A commercial Cu plate (B-60-P05) was purchased from Yamamoto MS Co., Ltd., Tokyo, Japan.

2.2. Selection of Appropriate Solvent for CNT Dispersion

A dispersibility test was conducted to select a suitable solvent for the CNT dispersion; 50 mL of numerous solvents, which were distilled water, ethanol, NMP, DSMO, DMF, acetonitrile, benzene, and 1.2 g/L sodium polyacrylate aqueous solution, were put into a glass vial together with 50 mg of CNTs and ultrasonicated in an ultrasonic bath (US-1R, 55 W, 40 kHz, AS ONE Corporation, Osaka, Japan) for 1 h. After ultrasonication, the suspension was transferred to a 50 mL centrifuge tube and centrifuged at 1000 rpm for 1 h using a centrifuge (CN-2060, AS ONE Corporation, Japan). Thereafter, the upper part of the suspension was transferred to a quartz cell using a pipette, and the absorbance was measured using a UV–vis spectrophotometer (UV-2450, Shimadzu Co., Kyoto, Japan) to confirm the dispersibility.

2.3. Bath Preparation and Electrodeposition of Cu and Cu/CNTs Composite Platings

NMP was selected as the solvent for the Cu and Cu/CNT composite plating baths based on the results of the dispersibility test. Typically, KI (75 mmol) was first completely dissolved in NMP and then CuI (75 mmol) was added, followed by mixing via magnetic stirring. After the CuI had dissolved completely, the total volume of the bath was adjusted to 250 mL for the Cu plating bath and 200 mL for the Cu/CNT composite plating bath using NMP. To obtain the same total bath volume of 250 mL, 50 mL NMP containing dispersed CNTs (the result of the dispersibility test introduced in Section 2.2) was added to the aforementioned 200 mL solvent for Cu/CNT composite plating. The bath was transferred into a 500 mL separable flask with rubber caps, and a three-electrode system was constructed for electrodeposition; a platinum (Pt) coil as the counter electrode (C.E.), Pt wire as the reference electrode (R.E.), and Cu plate as the working electrode (W.E.) were connected to a potentiostat/galvanostat (HZ-5000, Hokuto Denko Corporation, Tokyo, Japan). The Cu plate was masked with insulation tape (NITOFLON™, Nitto Denko Corporation, Osaka, Japan) to fix the electrodeposition area to 1 × 1 cm. Because of the high hygroscopicity of NMP, KI and CuI were vacuum-dried for 24 h before adding them to NMP, and electrolysis was conducted under Ar flow to prevent deterioration of the solvent by the adsorption of

moisture. The bath was continuously stirred using a magnetic stirrer during electrodeposition, and no aggregation of CNT was observed. After the electrodeposition was completed, the plates were sonicated for 1 min in KI solution, rinsed with distilled water, and finally dried using a heat gun.

A schematic of the experimental apparatus for electrodeposition is presented in Figure 1.

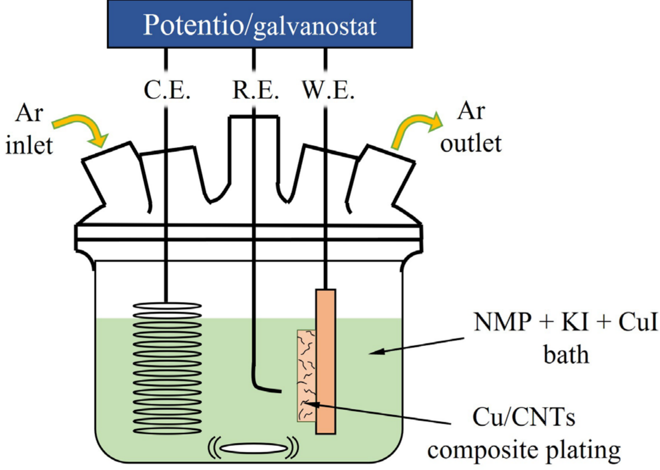

Figure 1. Schematic of the electrolysis cell.

2.4. Characterization

The microstructures of the CNTs and platings were observed using a field-emission scanning electron microscope (FE-SEM; JSM-6330F, JEOL, Tokyo, Japan).

The current efficiency: C_{eff}, was calculated as

$$C_{eff} \approx \frac{\Delta m \times n \times F}{M \times I \times t} \times 100, \quad (1)$$

where Δm is the weight of the electrodeposited film, defined as the weight change after electrodeposition (g); n is the ionic valence of Cu(I); F is the Faraday constant (C/mol); M is the atomic weight of Cu (g/mol); I is the applied electric current (A); and t is the electrodeposition time (s).

The amount of CNTs incorporated into the Cu/CNT composite plating was determined using a carbon/sulfur analyzer (EMIA-510, Horiba, Kyoto, Japan). The CNT content C_c (mass%) of the Cu/CNT composite plating was calculated as follows:

$$C_c \approx M_c = \frac{(M_t \times m_t) - (M_{Cu} \times m_{Cu})}{\Delta m} \times 100, \quad (2)$$

where M_c is the carbon content of the Cu/CNT composite plating (mass%); M_t and m_t are the total carbon content measured using a carbon/sulfur analyzer (mass%) and total weight (g) of the sample (including both the Cu substrate and plating), respectively; and M_{Cu} and m_{Cu} are the measured carbon content (mass%) and weight (g) of the Cu substrate, respectively.

The anticorrosion properties of Cu and Cu/CNT plating were evaluated by an anodic polarization test in 3 mass% NaCl solution. The test solution was degassed with Ar for 30 min to remove the dissolved oxygen before use. Plating samples are masked with insulating tape except for a 1 × 1 cm area. The measurement was performed from −0.3 V (vs. open circuit potential) to the anodic potential direction until +1.0 V (vs. Ag/AgCl) at a scan rate of 1 mV/s. All measurements were conducted after stabilizing open circuit potential for 1 h.

3. Results and Discussion

3.1. CNT Dispersibility Test

The various types of non-aqueous solvents are classified according to their properties. CNTs are well dispersed in polar aprotic solvents [40]. Therefore, we selected several solvents based on their properties, and the dispersibility of CNTs in these solvents were investigated. Solvents were classified into three types: polar protic solvents (water and ethanol), polar aprotic solvents (NMP, DMF, DMSO, and acetonitrile), and nonpolar solvents (benzene). The FE-SEM image of the CNTs used in this study is shown in Figure 2a. CNTs with diameters of approximately 10 nm tangled and formed aggregates. Suspensions containing CNTs (1.0 g/L of CNTs) were prepared in each solvent and sonicated for 1 h to disaggregate and disperse the CNTs. To confirm the degree of disaggregation, undispersed aggregated CNTs were sedimented by centrifugation, and the absorbance spectra of the supernatants containing the dispersed CNTs were recorded. The measurement results are shown in Figure 2b. A higher absorbance indicates the presence of a larger amount of dispersed CNTs. When polar aprotic solvents, such as NMP or DMF, were used, a black suspension remained after centrifugation (Figure 2c). Moreover, the absorbance was high throughout the measured wavelength range, indicating a good dispersion of the CNTs. This implies that polar aprotic solvents enable the disaggregation and dispersion of CNTs. In particular, the NMP showed the highest dispersibility among the solvents considered in this study. However, when water, ethanol, or benzene was used as the solvent, the CNTs settled at the bottom of the centrifuge tube after centrifugation (Figure 2d), and the absorbance spectra of the supernatants remained primarily in the background, indicating that no CNTs appeared in the supernatants. This was supported by the transparent appearance of the supernatant, as shown in Figure 2d. Based on these results, we selected NMP as a solvent for the Cu/CNT composite plating bath.

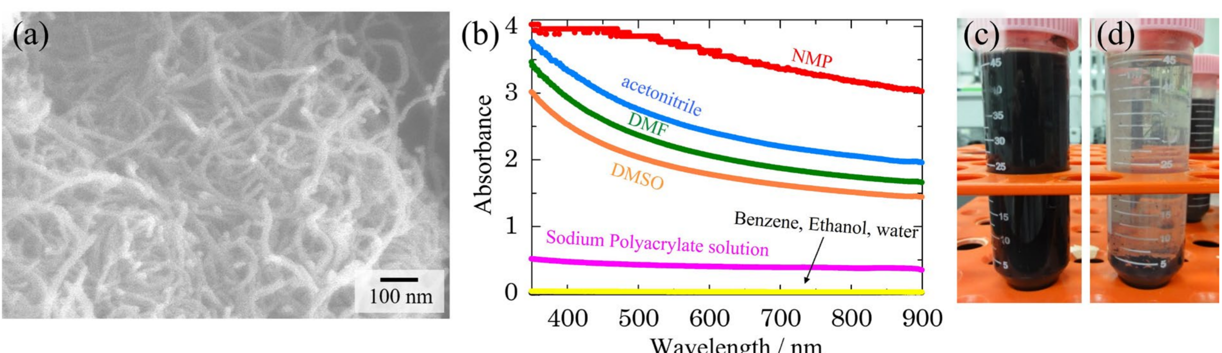

Figure 2. (**a**) SEM image of the used CNTs, (**b**) absorbance of CNT-dispersed solvent, and photographs of centrifuged suspensions: (**c**) NMP with 1 g/L of CNTs, and (**d**) ethanol with 1 g/L of CNTs.

3.2. Electrodeposition of Cu and Cu/CNTs Composite Plating

Subsequently, we investigated the electrodeposition behavior of Cu in NMP. The solubility of $CuSO_4$, which is a common Cu salt used in aqueous baths, is extremely low at NMP. Also, corrosion of the Cu substrate occurred spontaneously when $CuCl_2$ was used as the Cu ion source due to a comproportionation reaction, anticipated as follows:

$$CuCl_2 + Cu \leftrightarrow 2Cu^+ + 2Cl^- \quad (3)$$

Therefore, we considered using salts to form stable Cu complexes in the bath. We found that at least up to 0.4 mol/L KI is soluble in the NMP solvent, and equimolar amounts of CuI with KI could be further dissolved in this solvent, even though CuI alone barely dissolved. By adding KI and CuI to the NMP solvent, part of the added CuI formed a complex ion as follows:

$$CuI + xI^- \leftrightarrow CuI_{x+1}^{x-} \quad (4)$$

Possible copper–iodine complexes can be CuI^{2-}, $CuI_3{}^{2-}$, and $CuI_4{}^{3-}$. Because CuI alone showed low solubility in NMP, the formation of these complexes must have played an important role in the dissolution of the Cu salt. Such complexes were anticipated to have allowed the formation of the following complex ion with NMP:

$$CuI_x^{(x-1)-} + NMP \leftrightarrow \left[Cu - NMP\right]^+_{complex} + xI^- \tag{5}$$

Here, the Cu ions form a complex with NMP and become stable in the solvent. The existence of the Cu(I)–NMP complex has been reported previously [41]; therefore, a similar complex must have been formed in this study.

Figure 3a shows the cathodic polarization curve measured in NMP solvent containing 0.3 mol/L of CuI and 0.3 mol/L of KI. The cathodic current started to increase from −0.7 V, which corresponds to a reduction reaction of Cu. The reduction of Cu in the NMP-KI-CuI bath can be considered to proceed via two reactions:

$$CuI_x^{(x-1)-} + e^- \rightarrow Cu + xI^- \tag{6}$$

$$\left[Cu - NMP\right]^+_{complex} + e^- \rightarrow Cu + NMP \tag{7}$$

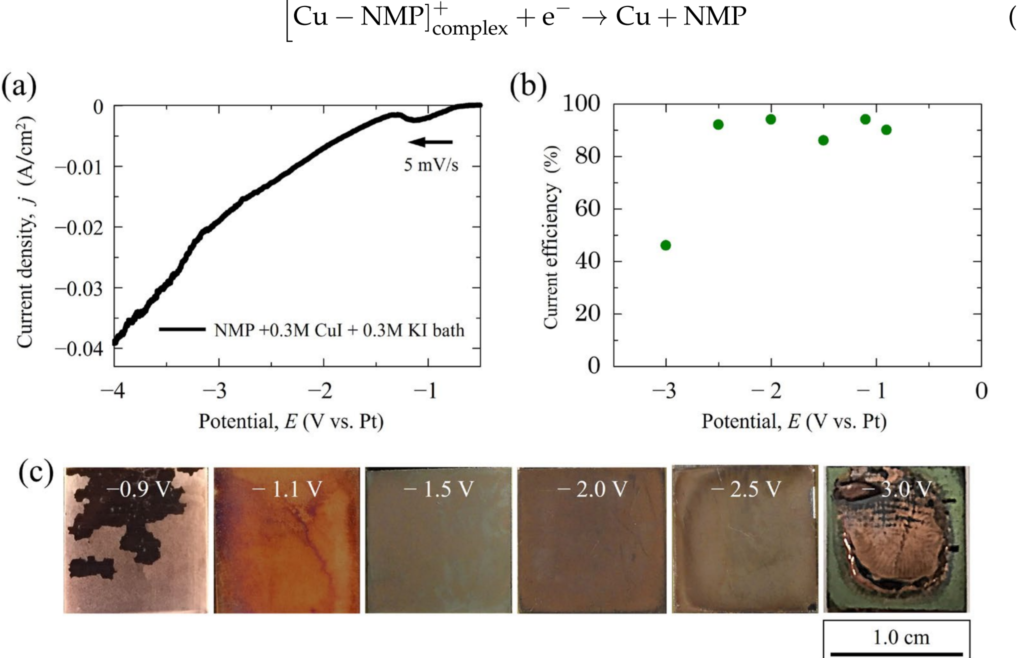

Figure 3. Electrodeposition behavior of Cu from NMP-KI-CuI bath: (**a**) Cathodic polarization curve, (**b**) current efficiency, and (**c**) photographs of Cu plating after constant potential electrolysis at respective potentials.

Therefore, constant potential electrolysis was conducted at potentials of −0.9, −1.1, −1.5, −2.0, −2.5, and −3.0 V to confirm the quality of Cu deposits. The calculated current efficiencies and photographs of the plated specimens are shown in Figure 3b,c, respectively. The current efficiency of Cu plating was close to 90%, and metallic plating was obtained when electrolysis was conducted at a potential range of −0.9 to −2.5 V. However, the Cu plating obtained at a potential of −0.9 V was fragile and partially ripped off by washing, as can be seen from the dark parts in Figure 3c. Meanwhile, the current efficiency drastically decreased to 43% at −3.0 V, and only the edges of the substrate were partially plated by Cu. Therefore, the potential range of −1.1 to −2.5 V was considered as the appropriate deposition potential range of Cu from this bath.

A Cu/CNT composite bath was prepared by adding 1.0 g/L of CNTs to the same NMP-KI-CuI bath and ultrasonicating it for 1 h. The added CNTs can be uniformly dispersed in

the plating bath without aggregation by ultrasonic dispersion. The cathodic polarization curve was measured in the Cu/CNT bath and plotted against that in the Cu bath, as shown in Figure 4. The addition of CNTs did not significantly hinder Cu reduction. The cathodic polarization slightly decreased after adding 1.0 g/L of CNTs to the Cu plating bath. The decrease in cathodic polarization is assumed to be due to the following two reasons [2,31]:

(i) Increased Cu ion concentration near the cathode surface by adding CNTs.
(ii) Increased conductivity at the cathode surface by adsorbed highly-conductive CNTs.

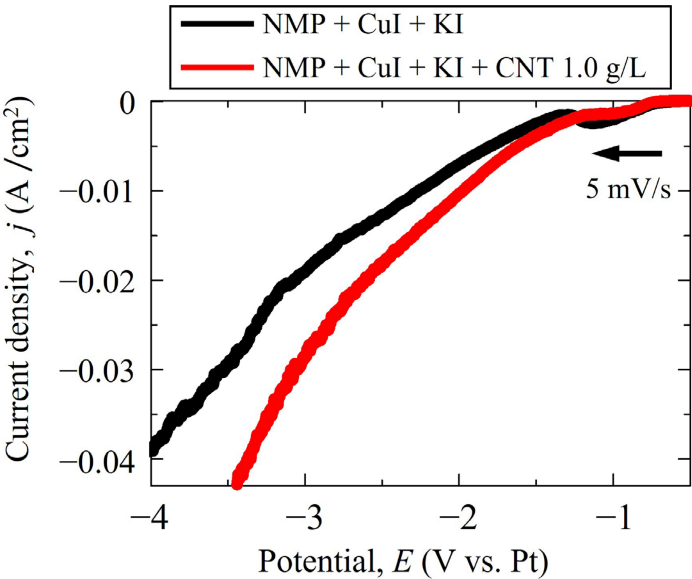

Figure 4. Cathodic polarization curves measured from Cu and Cu/CNTs bath.

As for (i), because metal ions can be adsorbed on the CNT surface [42], most of the Cu ions that exist as complex ions with NMP in the bath can be adsorbed onto the cathode surface together with the CNTs. In addition, for (ii), the cathodic polarization could be decreased because CNTs with high electrical conductivity were adsorbed on the cathode, and the plating surface area locally increased in the area where the CNTs were adsorbed.

3.3. Effect of Current Density

The quality of the deposits is significantly affected by the current density during electrolysis [43]. Therefore, the effect of current density on the quality of the Cu/CNT composite was investigated. The stirring rate was fixed at 250 rpm, and current density was varied from −2 to −20 mA/cm^2 considering the electrodeposition behavior of Cu based on cathodic polarization curves and the quality of constant potential-deposited plating specimens. In the case of Cu/CNT plating, the same current density range of −2 to −20 mA/cm^2 was applied since the cathodic polarization curves presented in Figure 4 did not show a significant difference with the addition of CNT in the Cu bath. Figure 5a shows the current efficiencies of the Cu and Cu/CNT composites deposited at various current densities. The results show that the current efficiency of Cu/CNT was lower than that of Cu under all current density conditions; however, interestingly, a similar trend was observed for both platings, wherein a high current efficiency was obtained at values of approximately −7 to −10 mA/cm^2. This corresponds to the optimum range of constant potential electrolysis expected from the cathodic potential curve shown in Figure 4. The calculated CNT content in the Cu/CNT composite is different, as shown in Figure 5b. The highest CNT content was obtained at −7 mA/cm^2, which is probably because the adsorbed CNTs at the cathode surface can be detached by stirring before being incorporated into the Cu matrix at lower current densities.

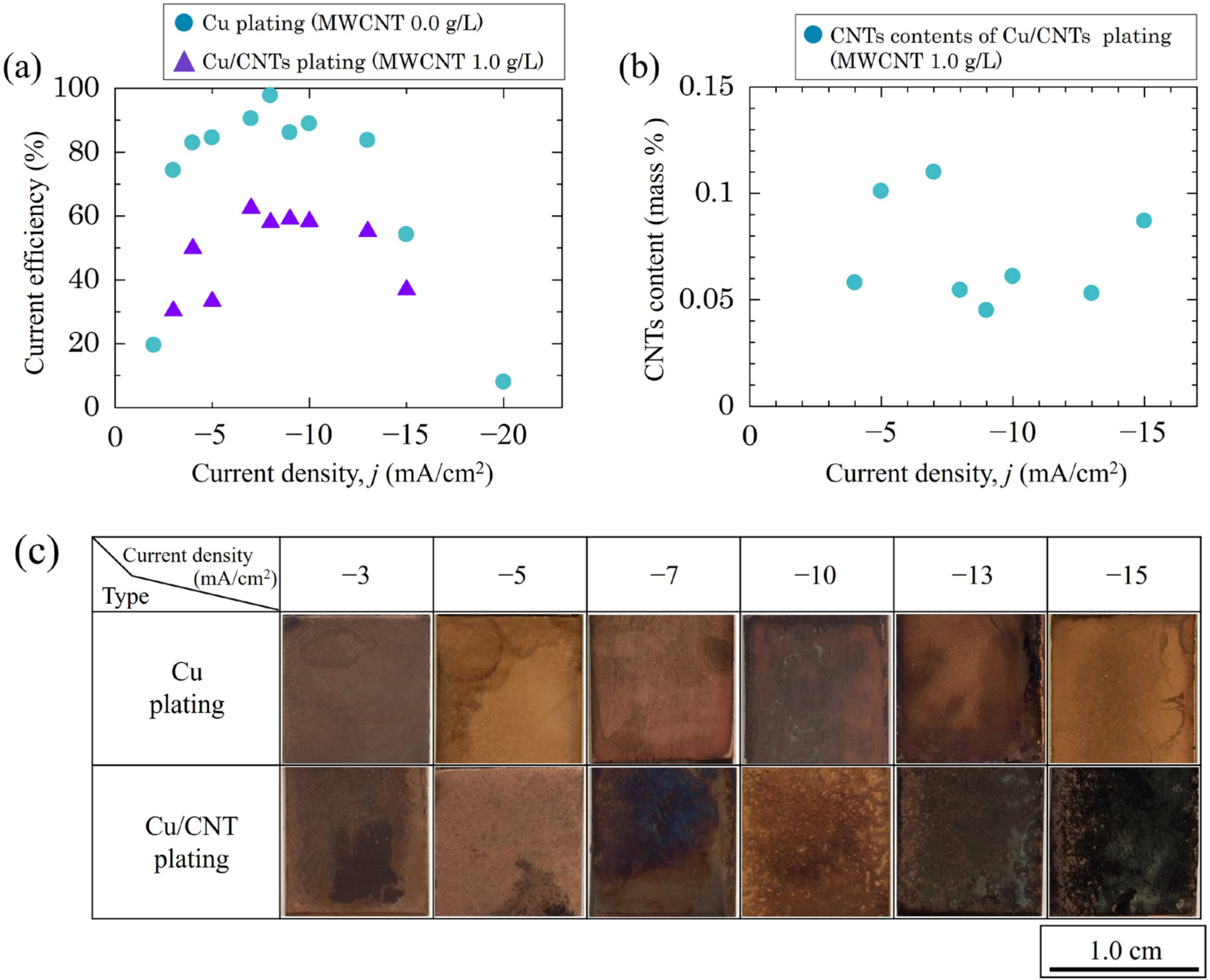

Figure 5. (**a**) Current efficiency of Cu and Cu/CNT plating; (**b**) CNT content of Cu/CNT plating at various current densities; and (**c**) photographs of plating specimens prepared using various current densities.

Figure 6 shows SEM images of the Cu and Cu/CNT composites deposited at current densities of −3, −7, and −10 mA/cm^2. The electrodeposition of the Cu plating at −3 mA/cm^2 resulted in the precipitation of coarse crystal grains, as shown in Figure 6a. In contrast, the plating deposited at current densities of −7 and −10 mA/cm^2 (Figure 6b,c) exhibited finer grains than those electrolyzed at −3 mA/cm^2. This can be attributed to the enhanced nucleation of Cu grains at higher current densities.

In the Cu/CNT composite platings, porous powdery deposits were obtained at a current density of −3 mA/cm^2 (Figure 6d), which was different from the appearance of the Cu platings without CNTs. At a low current density, the CNTs adsorbed on the plating surfaces are thought to be desorbed before being incorporated into the Cu matrix, leaving gaps where the CNTs are adsorbed. This caused changes in the morphology of the plated surfaces. Meanwhile, the current efficiency of the Cu/CNT composite platings reached a maximum of approximately 60% in the current density range of −7 to −10 mA, and a uniform deposition was obtained in this current density range (Figure 6e,f). Based on the above results, the appropriate range of current density for the electrodeposition of the Cu/CNT composites was determined to be −5 to −10 mA/cm^2.

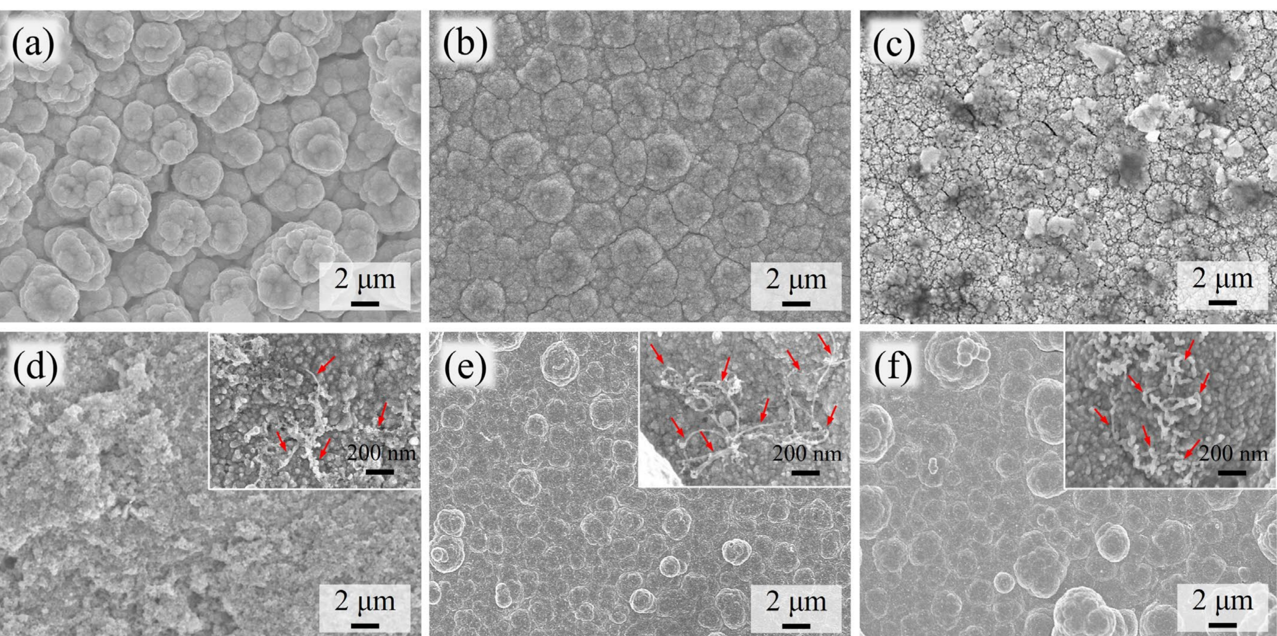

Figure 6. Surface SEM images for Cu (**a**–**c**) and Cu/CNT platings (**d**–**f**) deposited at a current density of (**a**,**d**) -3 mA/cm^2, (**b**,**e**) -7 mA/cm^2, and (**c**,**f**) -10 mA/cm^2. Inset images in (**d**–**f**) show respective high-magnification images and red arrows indicate codeposited CNTs.

3.4. Effects of Stirring Rate

In composite platings, the purpose of stirring is to maintain the suspended state of the particles and promote the supply of metal ions and particles to the electrode surface. Several studies have reported that the stirring rate has a significant effect on the particle content and quality of the deposits [44]. The effects of the stirring rate at current densities of -5, -7, and -10 m/cm^2 on the current density and CNT content of the Cu/CNT composites were investigated.

Figure 7a shows that the current efficiency decreases slightly as the stirring rate increases for both the Cu and Cu/CNT composite platings. The MWCNT content of the Cu/CNTs reached its highest value at 250 rpm, as shown in Figure 7b. When the stirring rate is lower than 250 rpm, the supply of MWCNTs to the electrode surface may be insufficient, and particles may be rapidly detached from the cathode surface before being incorporated in the Cu layer when the stirring rate is higher than 250 rpm.

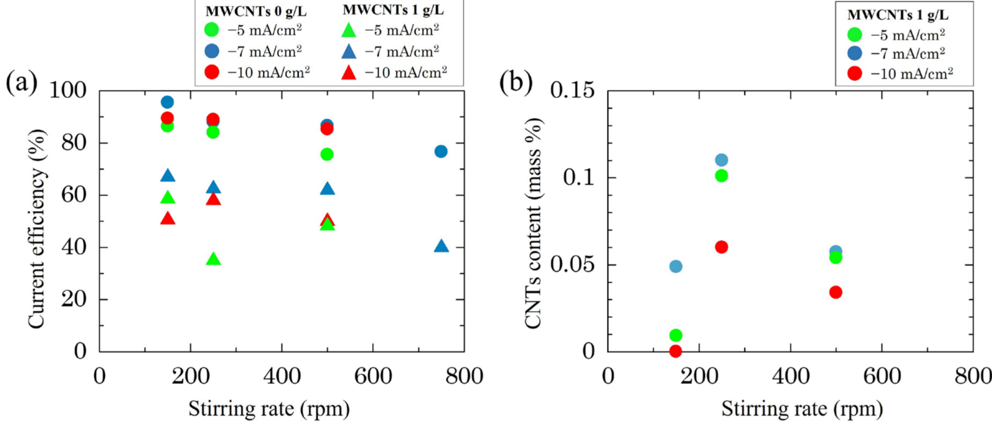

Figure 7. (**a**) Effect of the stirring rate on the current efficiency of Cu and Cu/CNT platings; and (**b**) CNT content of Cu/CNT composite platings at various stirring rates.

3.5. Effect of Pulse Electrodeposition

The maximum CNT content of the Cu/CNT composite platings obtained by constant current electrolysis is 0.12 mass%. Therefore, pulsed electrolysis was conducted to improve the uniformity of the deposits and increase the CNT content. Pulse electrodeposition can reduce the thickness of the diffusion layer at the interface of the cathode, allowing a higher current density to be applied, and thereby improving the quality of the deposits through uniformization and crystal refinement during electrodeposition [45].

As for the electrolysis conditions, the on-time and duty ratio were fixed at 0.1 s and 0.2, respectively (on-time: 0.1 s, off-time: 0.4 s), and the current densities during on-time were varied as −20, −30, and −50 mA/cm^2. Table 1 summarizes the CNT content and current efficiency of the Cu and Cu/CNT composite platings under each current density condition. Similar to the results obtained from constant current electrolysis, it was confirmed that the incorporation of CNTs into the Cu matrix lowered the current efficiency. At a current density of −30 mA/cm^2, a maximum CNT content of 0.22 mass% was obtained, which is higher than the maximum CNT content of 0.12 mass% of the Cu/CNT composite platings deposited via constant current electrolysis at −7 mA/cm^2. However, The CNT content obtained in this study was slightly lower than that of the Cu/CNT composite plating (maximum 0.55 mass% by constant current deposition [31] and 0.59 mass% by pulse-reverse deposition [32]) obtained from the sulfuric copper based aqueous bath using polyacrylic acid as a dispersant. Pulse electrodeposition under adequate conditions appeared to be effective in improving the CNT content of the Cu/CNT composite platings.

Table 1. CNT contents and current efficiency of Cu/CNT composite platings prepared by pulse electrolysis at various current densities (stirring rate: 250 rpm, CNT concentration of bath: 1.0 g/L, duty ratio: 0.2).

Current Density [mA/cm^2]	MWCNT Content [wt%]	Current Efficiency [%]
	Cu platings	
−20	-	70
−30	-	76
−50	-	77
	Cu/CNT composite platings	
−20	0.09	52
−30	0.22	26
−50	Below detection limit	45

Figure 8 shows SEM images and photographs of the Cu and Cu/CNT composite platings deposited at the same pulse current density of −30 mA/cm^2. The SEM image of the Cu plating in Figure 8a shows a dense metallic precipitate structure, and the appearance of the plating is close to that of pure metallic Cu. In contrast, the SEM image of the Cu/CNT composite plating containing 0.22 mass% of CNTs shows a rough surface with a small grain size. Pulsed electrodeposition in the presence of CNTs significantly enhanced nucleation. The pulsed electrodeposition possibly provided more grain boundaries for CNTs to be introduced while readily depositing enough Cu to trap the CNTs in the Cu matrix, leading to a higher CNT content.

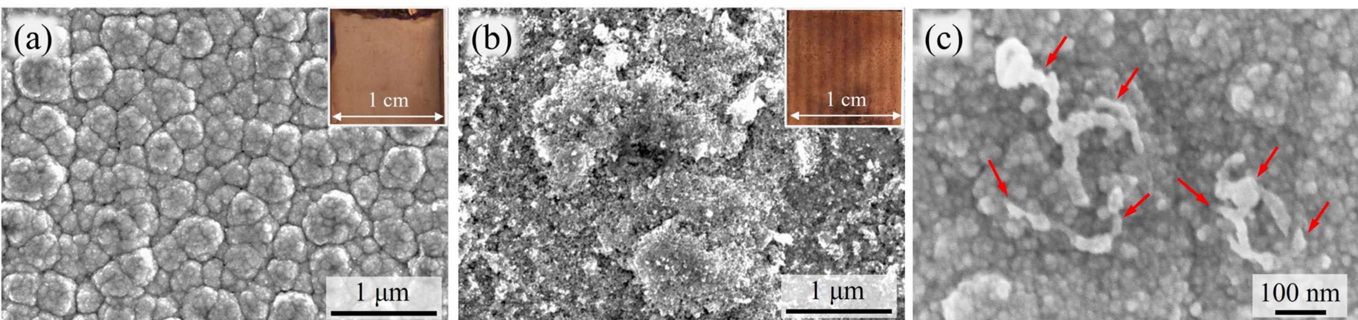

Figure 8. SEM images and photographs for pulse-deposited (**a**) Cu and (**b**) Cu/CNT composite platings; (**c**) shows high-magnification image of (**b**) and yellow colored arrows indicate codeposited CNTs. The pulse current density was −30 mA/cm^2.

3.6. Anticorrosion Properties

Anodic polarization curves are measured in 3 mass% NaCl solution to evaluate the corrosion resistance of Cu and Cu/CNT plating, and the results are plotted in Figure 9. The corrosion potential (E_{corr}) of Cu and Cu/CNT plating are −402 and −393 mV, respectively, which slightly shifted towards noble potential direction by co-deposition of CNT into Cu plating. Co-deposition of carbon materials into metal plating can shift the E_{corr} toward noble potential direction and is also effective in decreasing the (I_{corr}) of the plating [2,46]. The calculated I_{corr} by Tafel's equation was 59.7 and 29.6 μA/cm^2 respectively, indicating that the Cu/CNT plating has better anticorrosion properties than the Cu plating. Polarization parameters are summarized in Table 2.

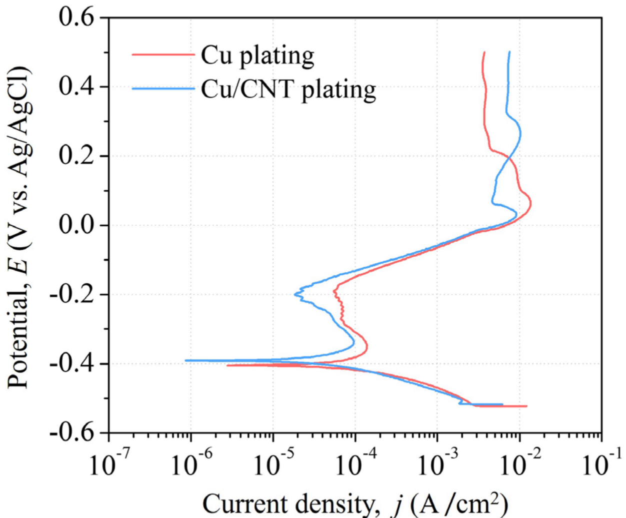

Figure 9. Anodic polarization curves for Cu and Cu/CNT plating measured in 3 mass% NaCl solution. Both platings are prepared by a pulse current density of −30 mA/cm^2.

Table 2. Polarization parameters for Cu and Cu/CNT plating: corrosion potential (E_{corr}), corrosion current density (I_{corr}), anodic Tafel's slope (β_a), and cathodic Tafel's slope (β_c).

Specimens	E_{corr} (mV)	I_{corr} (μA/cm^2)	β_a (mV)	β_c (mV)
Cu plating	−402	59.7	96.2	48.2
Cu/CNT plating	−393	29.6	85.1	42.5

4. Conclusions

In this study, the electrodeposition of Cu/CNT composite plating in a non-aqueous solution was evaluated as a method for dispersing hydrophobic CNTs in the plating so-

lution without any chemical treatment of CNTs or using additional chemical dispersants in the plating bath. NMP, which is a polar aprotic solvent, was selected as the solvent for Cu/CNT deposition based on the CNT dispersion test results; it was confirmed that the electrodeposition of Cu was possible without corrosion of the substrate from a bath containing KI and CuI by forming stable Cu complex ions. The potential range where uniform Cu deposits were obtained was approximately −1.0 to −2.5 V, and a high current efficiency of approximately 90% was obtained at this potential. However, the codeposition of CNTs decreased the current efficiency to approximately 60%. In constant current electrodeposition, a Cu/CNT composite plating containing a maximum of 0.12 mass% of CNTs was obtained at a current density of −7 mA/cm^2 and a stirring speed of 250 rpm using a bath with 1.0 g/L-CNTs. Furthermore, by applying pulse electrodeposition, a Cu/CNT composite plating containing a maximum of 0.22 mass% of CNTs was obtained at a pulse current density of −30 mA/cm^2. In addition, Cu/CNT showed a slightly higher E_{corr} (−393 mV) and lower I_{corr} (29.6 μA/cm^2) than Cu plating, suggesting that codeposition of CNT is also effective in improving the anticorrosion resistance of electrodeposited Cu. This study confirmed the possibility of fabricating a Cu/CNT composite plating in an NMP solvent, and provides useful guidelines for the electrodeposition of metal/carbon composite plating in nonaqueous solutions.

Author Contributions: Conceptualization, R.I.; Methodology, Y.F.; Validation, J.-H.P. and T.H.; Formal analysis, Y.F.; Investigation, Y.F. and J.-H.P.; Resources, Y.K.; Data curation, T.H.; Writing —Original Draft Preparation, J.-H.P. and T.H.; Writing—Review and Editing, V.P.; Visualization, J.-H.P. and V.P.; Supervision, T.B. and R.I.; Project Administration, T.H. and R.I.; Funding Acquisition, R.I. All authors have read and agreed to the published version of the manuscript.

Funding: This research was partially funded by the Japan Science and Technology Agency (JST)-OPERA (grant number JPMJOP1843).

Institutional Review Board Statement: Not applicable.

Informed Consent Statement: Not applicable.

Data Availability Statement: Data is contained within the article.

Acknowledgments: This work was partially supported by the JST-OPERA Program, Japan [grant number JPMJOP1843].

Conflicts of Interest: The authors declare no conflict of interest.

References

1. Qu, X.; Zhang, L.; Wu, M.; Ren, S. Review of metal matrix composites with high thermal conductivity for thermal management applications. *Prog. Nat. Sci. Mater. Int.* **2011**, *21*, 189–197. [CrossRef]
2. Park, J.H.; Hagio, T.; Ichino, R. Improvement in the corrosion resistance of electrodeposited Ni-W alloy by MWCNT co-deposition and prevention of metal-carbon interfacial corrosion by carbide formation. *J. Alloys Compd.* **2023**, *939*, 168788. [CrossRef]
3. Song, G.; Li, S.; Liu, G.; Fu, Q.; Pan, C. Influence of graphene oxide content on the Zn- Gr composite layer prepared by pulse reverse electro-plating. *J. Electrochem. Soc.* **2018**, *165*, D501. [CrossRef]
4. Park, J.H.; Wada, T.; Naruse, Y.; Hagio, T.; Kamimoto, Y.; Ichino, R. Electrodeposition of Ni-W/CNT composite plating and its potential as coating for PEMFC bipolar plate. *Coatings* **2020**, *10*, 1095. [CrossRef]
5. Tao, J.M.; Chen, X.F.; Hong, P.; Yi, J.H. Microstructure and electrical conductivity of laminated Cu/CNT/Cu composites prepared by electrodeposition. *J. Alloys Compd.* **2017**, *717*, 232–239. [CrossRef]
6. Hagio, T.; Park, J.H.; Naruse, Y.; Goto, Y.; Kamimoto, Y.; Ichino, R.; Bessho, T. Electrodeposition of nano-diamond/copper composite platings: Improved interfacial adhesion between diamond and copper via formation of silicon carbide on diamond surface. *Surf. Coat. Technol.* **2020**, *403*, 126322. [CrossRef]
7. Naruse, Y.; Park, J.-H.; Hagio, T.; Kamimoto, Y.; Bessho, T.; Ryoichi, I. Effect of SiC formation temperature on improvement in thermal conductivity of electrodeposited SiC-coated diamond/Cu composite plating. *Compos. Interfaces* **2021**, *29*, 256–273. [CrossRef]
8. Cui, R.; Han, Y.; Zhu, Z.; Chen, B.; Ding, Y.; Zhang, Q.; Wang, Q.; Ma, G.; Pei, F.; Ye, Z. Investigation of the structure and properties of electrodeposited Cu/graphene composite coatings for the electrical contact materials of an ultrahigh voltage circuit breaker. *J. Alloys Compd.* **2019**, *777*, 1159–1167. [CrossRef]
9. Arai, S. Fabrication of metal/carbon nanotube composites by electrochemical deposition. *Electrochem* **2021**, *2*, 563–589. [CrossRef]

10. Yang, Y.L.; Wang, Y.D.; Ren, Y.; He, C.S.; Deng, J.N.; Nan, J.; Chen, J.G.; Zuo, L. Single-walled carbon nanotube-reinforced copper composite coatings prepared by electrodeposition under ultrasonic field. *Mater. Lett.* **2008**, *62*, 47–50. [CrossRef]
11. Kamimoto, Y.; Ohkura, S.; Hagio, T.; Wada, T.; Tanaka, H.; Hara, H.; Deevanhxay, P.; Ichino, R. Nickel–carbon composite plating using a Watts nickel electroplating bath. *SN Appl. Sci.* **2020**, *2*, 170. [CrossRef]
12. Arai, S.; Endo, M. Carbon Nanofiber-Copper Composites Fabricated by Electroplating. *Electrochem. Solid-State Lett.* **2004**, *7*, C25. [CrossRef]
13. Arai, S.; Endo, M. Various carbon nanofiber–copper composite films prepared by electrodeposition. *Electrochem. Commun.* **2005**, *7*, 19–22. [CrossRef]
14. Shimizu, M.; Ogasawara, T.; Ohnuki, T.; Arai, S. Multi-layered copper foil reinforced by co-deposition of single-walled carbon nanotube based on electroplating technique. *Mater. Lett.* **2020**, *261*, 126993. [CrossRef]
15. Li, S.; Song, G.; Zhang, Y.; Fu, Q.; Pan, C. Graphene-reinforced Zn–Ni alloy composite coating on iron substrates by pulsed reverse electrodeposition and its high corrosion resistance. *ACS Omega* **2021**, *6*, 13728–13741. [CrossRef]
16. Xiang, L.; Shen, Q.; Zhang, Y.; Bai, W.; Nie, C. One-step electrodeposited Ni-graphene composite coating with excellent tribological properties. *Surf. Coat. Technol.* **2019**, *373*, 38–46. [CrossRef]
17. Wu, Y.; Sun, Y.; Luo, J.; Cheng, J.; Wang, Y.; Wang, H.; Ding, G. Microstructure of Cu-diamond composites with near-perfect interfaces prepared via electroplating and its thermal properties. *Mater. Charact.* **2019**, *150*, 199–206. [CrossRef]
18. Zhang, Y.; Feng, L.; Qiu, W. Enhancement of the wear resistance of Ni-diamond composite coatings via glycine modification. *Diam. Relat. Mater.* **2020**, *109*, 108086. [CrossRef]
19. Li, B.; Mei, T.; Chu, H.; Wang, J.; Du, S.; Miao, Y.; Zhang, W. Ultrasonic-assisted electrodeposition of Ni/diamond composite coatings and its structure and electrochemical properties. *Ultrason. Sonochem.* **2021**, *73*, 105475. [CrossRef]
20. Ning, D.; Zhang, A.; Wu, H. Enhanced wear performance of Cu-carbon nanotubes composite coatings prepared by jet electrodeposition. *Materials* **2019**, *12*, 392. [CrossRef]
21. Arora, S.; Kumari, N.; Srivastava, C. Microstructure and corrosion behaviour of NiCo-carbon nanotube composite coatings. *J. Alloys Compd.* **2019**, *801*, 449–459. [CrossRef]
22. Arora, S.; Sharma, B.; Srivastava, C. ZnCo-carbon nanotube composite coating with enhanced corrosion resistance behavior. *Surf. Coat. Technol.* **2020**, *398*, 126083. [CrossRef]
23. Rekha, M.Y.; Kamboj, A.; Srivastava, C. Electrochemical behavior of SnNi-graphene oxide composite coatings. *Thin Solid Film.* **2018**, *653*, 82–92. [CrossRef]
24. Arora, S.; Srivastava, C. Microstructure and corrosion properties of NiCo-graphene oxide composite coatings. *Thin Solid Film.* **2019**, *677*, 45–54. [CrossRef]
25. Li, D.; Xue, J.; Zuo, T.; Gao, Z.; Xiao, L.; Han, L.; Li, S.; Yang, Y. Copper/functionalized-carbon nanotubes composite films with ultrahigh electrical conductivity prepared by pulse reverse electrodeposition. *J. Mater. Sci. Mater. Electron.* **2020**, *31*, 14184–14191. [CrossRef]
26. Feng, Y.; McGuire, G.E.; Shenderova, O.A.; Ke, H.; Burkett, S.L. Fabrication of copper/carbon nanotube composite thin films by periodic pulse reverse electroplating using nanodiamond as a dispersing agent. *Thin Solid Film.* **2016**, *615*, 116–121. [CrossRef]
27. Arai, S.; Fukuoka, R. A carbon nanotube-reinforced noble tin anode structure for lithium-ion batteries. *J. Appl. Electrochem.* **2016**, *46*, 331–338. [CrossRef]
28. Shimizu, M.; Ohnuki, T.; Ogasawara, T.; Banno, T.; Arai, S. Electrodeposited Cu/MWCNT composite-film: A potential current collector of silicon-based negative-electrodes for Li-Ion batteries. *RSC Adv.* **2019**, *9*, 21939. [CrossRef]
29. Chen, X.; Tao, J.; Yi, J.; Li, C.; Bao, R.; Liu, Y.; You, X.; Tan, S. Balancing the strength and ductility of carbon nanotubes reinforced copper matrix composites with microlaminated structure and interdiffusion interface. *Mater. Sci. Eng. A* **2018**, *712*, 790–793. [CrossRef]
30. Zhou, M.; Mai, Y.; Ling, H.; Chen, F.; Lian, W.; Jie, X. Electrodeposition of CNTs/copper composite coatings with enhanced tribological performance from a low concentration CNTs colloidal solution. *Mater. Res. Bull.* **2018**, *97*, 537–543. [CrossRef]
31. Arai, S.; Saito, T.; Endo, M. Cu–MWCNT composite films fabricated by electrodeposition. *J. Electrochem. Soc.* **2010**, *157*, D147–D153. [CrossRef]
32. Arai, S.; Suwa, Y.; Endo, M. Cu/Multiwalled carbon nanotube composite films fabricated by pulse-reverse electrodeposition. *J. Electrochem. Soc.* **2011**, *158*, D49–D53. [CrossRef]
33. Arai, S.; Kato, A. Mechanism for codeposition of multiwalled carbon nanotubes with copper from acid copper sulfate bath. *J. Electrochem. Soc.* **2013**, *160*, D380–D385. [CrossRef]
34. Fu, S.; Chen, X.; Liu, P.; Liu, W.; Liu, P.; Zhang, K.; Chen, H. Electrodeposition and properties of composites consisting of carbon nanotubes and copper. *J. Mater. Eng. Perform.* **2018**, *27*, 5511–5517. [CrossRef]
35. Wang, M.; Yang, X.; Tao, J.; Bub, Y.; Liu, Y.; Pu, Z.; Yi, Y. Achieving high ductility in layered carbon nanotube/copper composite prepared by composite electrodeposition. *Diam. Relat. Mater.* **2020**, *108*, 107992. [CrossRef]
36. Aliyu, A.; Srivastava, C. Correlation between growth texture, crystallite size, lattice strain and corrosion behavior of copper-carbon nanotube composite coatings. *Surf. Coat. Technol.* **2021**, *405*, 126596. [CrossRef]
37. Qin, X.; Liu, J.; Wang, F.; Ji, J. Effect of multi-walled carbon nanotubes as second phase on the copper electrochemical reduction behavior for fabricating their nanostructured composite films. *J. Electroanal. Chem.* **2011**, *651*, 233–236. [CrossRef]

38. Zheng, L.; Sun, J.; Chen, Q. Carbon nanotubes reinforced copper composite with uniform CNT distribution and high yield of fabrication. *Micro. Nano. Lett.* **2017**, *12*, 722–725. [CrossRef]
39. Pech-Rodríguez, W.J.; Rocha-Rangel, E.; Calles-Arriaga, C.A.; Vargas-Gutiérrez, G.; Rodríguez-Varela, F.J. Study of the electrophoretic deposition copper–carbon nanotubes composite coatings in deep eutectic solvent using a Taguchi experimental design approach. *Adv. Appl. Ceram.* **2018**, *117*, 461–467. [CrossRef]
40. Ausman, K.D.; Piner, R.; Lourie, O.; Ruoff, R.S.; Korobov, M. Organic solvent dispersions of single-walled carbon nanotubes: Toward solutions of pristine nanotubes. *J. Phys. Chem. B* **2000**, *104*, 8911–8915. [CrossRef]
41. Lou, J.; Zhan, Y. Single-Crystalline Metal Nanorings and Methods for Synthesis Thereof. U.S. Patent 8,460,428 B2, 11 June 2013.
42. Stafiej, A.; Pyrzynska, K. Adsorption of heavy metal ions with carbon nanotubes. *Sep. Purif. Technol.* **2007**, *58*, 49–52. [CrossRef]
43. Park, J.H.; Hagio, T.; Kamimoto, Y.; Ichino, R. Electrodeposition of a Novel Ternary Fe–W–Zn Alloy: Tuning Corrosion Properties of Fe–W Based Alloys by Zn Addition. *J. Electrochem. Soc.* **2020**, *167*, 132508. [CrossRef]
44. Wang, X.; Chou, C.C.; Lee, J.W.; Wu, R.; Chang, H.Y.; Ding, Y. Preparation and investigation of diamond-incorporated copper coatings on a brass substrate by composite electrodeposition. *Surf. Coat. Technol.* **2020**, *386*, 125508. [CrossRef]
45. Gou, R.; Park, J.H.; Yamashita, S.; Hagio, T.; Ichono, R.; Kita, H. Aluminum Electrodeposition on the Surface of Boron Carbide Ceramics by Use EMIC–$AlCl_3$ Ions Liquid. *Coatings* **2022**, *12*, 1535. [CrossRef]
46. Fan, Y.; He, Y.; Luo, P.; Shi, T.; Li, H. Pulse Current Electrodeposition and Characterization of Ni-W-MWCNTs Nanocomposite Coatings. *J. Electrochem. Soc.* **2015**, *162*, D270–D274. [CrossRef]

Disclaimer/Publisher's Note: The statements, opinions and data contained in all publications are solely those of the individual author(s) and contributor(s) and not of MDPI and/or the editor(s). MDPI and/or the editor(s) disclaim responsibility for any injury to people or property resulting from any ideas, methods, instructions or products referred to in the content.